17th World Conference on Earthquake Engineering, 17WCEE
Sendai, Japan - September 13th to 18th 2020

INITIAL DAMPING RATIO FOR THE SEISMIC DESIGN OF BUILDINGS

N. Nakamura[(1)], N. Satake[(2)], N. Ougiya[(3)], S. Ito[(4)]

[(1)] *Professor, Hiroshima University, naohiro3@hiroshima-u.ac.jp*
[(2)] *Engineer, Engineering & Risk Services, satake@ers-co.jp*
[(3)] *Researcher, Haseko Corporation, Narumi_Ougiya@haseko.co.jp*
[(4)] *Manager, Daiwa House Industry, ito-shinji@daiwahouse.jp*

Abstract

The damping characteristics of buildings are less elucidated than those of stiffness and mass. However, damping is known to significantly affect the dynamic response, behavior, and performance of buildings. The damping of buildings comprises two parts: 1) initial damping, which arises from the elastic condition, and 2) hysteretic damping, which seemingly relates to the nonlinear condition. This paper investigates the ratios of initial damping.

In the seismic design of Japanese high-rise buildings, damping ratios of 2% and 3% are often used for steel constructions and reinforced concrete (RC) structures, respectively. However, the reasons for selecting these values have not been fully elucidated.

To properly estimate damping parameters in the seismic design of buildings, the observation and estimation of the damping characteristics of actual buildings are essential. During a long-term study of building damping, a subcommittee of the Architectural Institute of Japan built and maintained a damping database. In 2000, after analyzing this database, the subcommittee proposed damping ratios (mainly against wind forces) for the structural design of buildings. At that time, the amplitudes of most of the observed data were comparatively small. As the damping amplitude influences the damping ratio, large-amplitude data generated by strong earthquakes are required to determine the appropriate damping ratios in the seismic design of buildings.

Since 2000, many large-amplitude data have been obtained, included that from the 2011 off the Pacific coast of Tohoku earthquake in Japan. Based on these data, this study investigates the ratios of initial damping for the seismic design of buildings.

The damping ratios of buildings vary depending on a building's height, with higher ratios for low-rise structures and lower ratios for high-rise buildings. This trend is attributed to the effect of the soil–structure interaction (SSI), which varies with soil conditions, foundation types, basement conditions, and other factors. Thus, only the data from high-rise buildings (with a natural period of over 1 s) are used herein, because these data can reveal building damping ratios without the SSI effect.

In addition, and to reduce data variability, the following characteristics of damping ratios were considered while selecting the observed data: 1) amplitude dependency and 2) experience of a previous large earthquake.

The obtained damping ratios are highly variable, as evidenced by their average values (avg.) and standard deviations (σ). The values are corrected for steel buildings, because damping ratios often decrease with increasing amplitude.

From this assessment, the following rounded ratios for the initial damping of buildings are proposed. These values should be applied according to the importance of the building.

RC/SRC buildings:	(Avg.): 2.0%,	(Avg. −0.5 σ): 1.5%,	(Avg. −1.0 σ): 1.0%
Steel buildings:	(Avg.): 1.5%,	(Avg. −0.5 σ): 1.0%,	(Avg. −1.0 σ): 0.5%

Keywords: Initial damping, Damping ratio, Seismic design, Buildings

1. Introduction

The physical properties of the damping of buildings are less elucidated than those of stiffness and mass; however, damping has a significant effect on the behavior of a building against dynamic external forces, such as earthquakes and wind. The damping of buildings comprises two parts:

1) initial damping, which arises from the elastic condition, and
2) hysteretic damping, which seemingly relates to the nonlinear condition.

This paper investigates the ratios of initial damping. In the seismic design of Japanese high-rise buildings, damping ratios of 2% and 3% for the horizontal direction are often used for steel (S) buildings and reinforced concrete (RC) buildings, respectively. However, the reasons for selecting these values have not been fully elucidated.

The Architectural Institute of Japan (AIJ) has collected and analyzed measured data on building damping since 1993 and has compiled a database (DB) of this information. In addition to the data from general buildings, other constructions, such as towers and shell structures, are also included. By analyzing this DB, the damping ratios for the structural design of buildings, mainly against wind forces, were proposed in 2000 [1], [2]. At that time, the amplitudes of most of the observed data were comparatively small. As the damping amplitude influences the damping ratios, large-amplitude data caused by strong earthquakes are crucial to determine the damping ratios for application in the seismic design of buildings. Since 2000, many large-amplitude data have been obtained, including that from the 2011 off the Pacific coast of Tohoku earthquake (hereafter referred to as the Tohoku earthquake).

The damping ratios of buildings vary depending on the building's height, with higher ratios for low-rise structures and lower ratios for high-rise buildings. This trend is attributed to the effect of the soil–structure interaction (SSI). This effect varies according to soil conditions, foundation types, basement conditions, and other factors. To establish the damping ratio of a building itself without the SSI effect, this study considered that an analysis using only high-rise building data was appropriate.

This paper analyzes the DB of general buildings, including buildings constructed from S, RC, and steel reinforced concrete (SRC). First, in Chapter 2, a trend analysis of the damping ratio is conducted using all data in the DB (382 buildings in total). Chapter 3 presents a trend analysis on the observation data from 59 buildings during the Tohoku earthquake. In Chapter 4, the average and standard deviations of these data are used to investigate the damping ratio of the building itself—excluding the influence of the SSI. Based on these studies, rounded ratios for the initial damping of buildings are proposed in Chapter 5. These suggested values should be used depending on the importance of the building.

2. Trend analysis using the entire DB

This chapter presents the results of a trend analysis of the damping ratio of all DB data based on [3] and [4]. The DB used for the trend analysis includes data quoted from documents published by the AIJ and others and observations from the Tohoku earthquake. The building data used for the trend analysis is for a total of 382 buildings, including 183 S buildings, 104 RC buildings, and 95 SRC buildings. Some SRC buildings include Concrete Filled Steel Tube (CFT) buildings. The actual measurements from the DB are divided into the short-side direction and the long-side direction. To examine the damping ratio in this study, each is treated as one data element. Therefore, the number of data is larger than the number of building data.

The types of observation records held in the DB comprise microtremor observation records (hereafter referred to as microtremor), observation records of manpower and forced excitation (hereafter referred to as forced excitation), and wind observation records (hereafter referred to as wind observation). Some records are based on earthquake observation records (hereafter referred to as earthquake observation). Therefore, in order to examine the amplitude dependency of the identification result of the damping ratio, the tendency of the damping ratio by each observation record is analyzed. The relationship between the magnitudes of the amplitudes is as follows: (microtremor) < (forced excitation) < (wind and earthquake observation); however, this analysis does not reveal specific amplitude values. Figs.1 and 2 present the relative frequency

distribution for the primary damping ratio and the relationship between the primary damping ratio and the primary natural frequency for S buildings and RC buildings, respectively. The relationship figures contain regression curves that correspond to each observation type using Equation (1). In the equation, T and h represent the natural period (s) and the damping ratio (%), respectively. The regression coefficients are a and b.

$$h(\%) = a / T + b \tag{1}$$

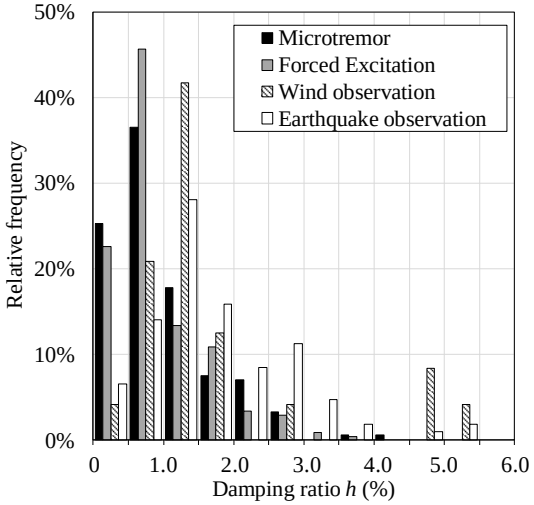

(a) Relative frequency bistribution

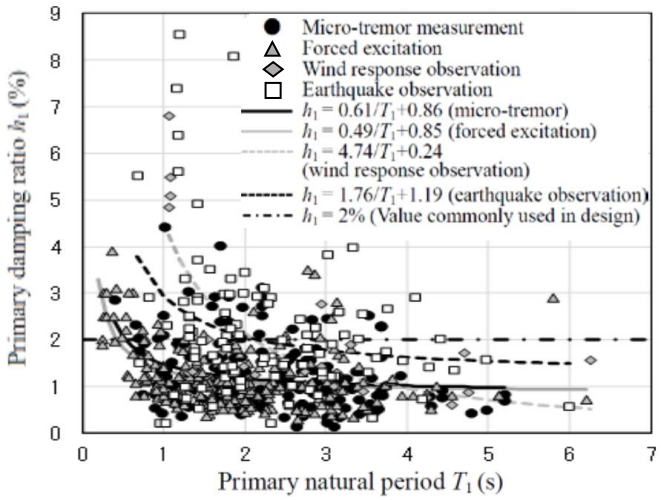

(b) Relationship between damping ratio and natural period

Fig.1 – S buildings

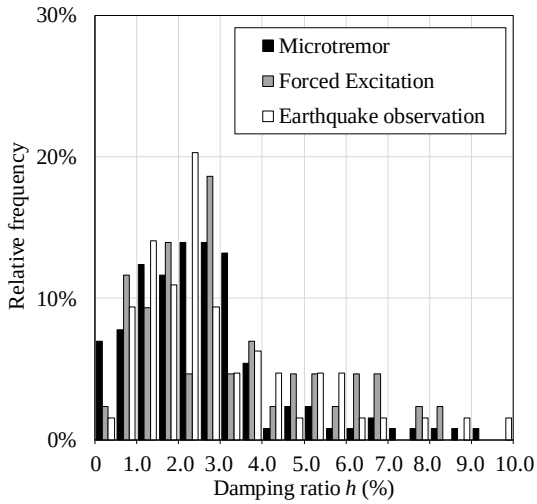

(a) Relative frequency bistribution

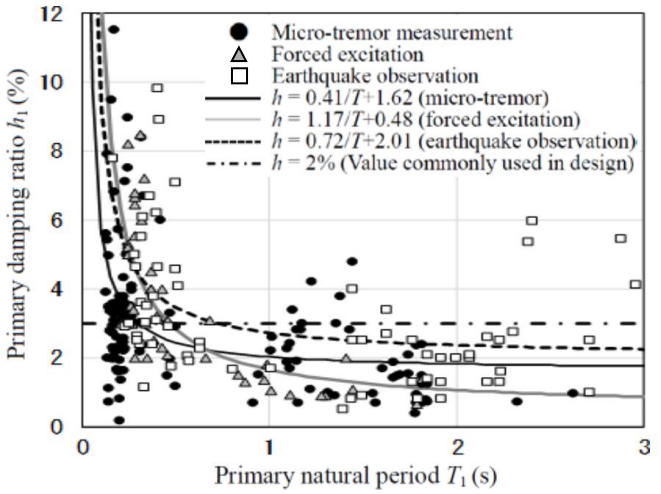

(b) Relationship between damping ratio and natural period

Fig.2 – RC buildings

The results of the trend analysis of S buildings presented in Fig. 1 (a) confirm that the microtremor and the forced excitation values tend to be relatively similar with distributions between 0% and 3% and their peaks are between 0.5% and 1.0%. Additionally, On the other hand, the damping ratio based on wind and

earthquake observations distribute widely and their peaks are about 1% to 1.5%; this is relatively high compared with the values for microtremor and forced excitation. The damping ratio over 3% almost consists of wind and earthquake observation. In Fig. 1 (b), the regression curve for earthquake observation is higher than those of for microtremor and forced excitation.

The results of the trend analysis of RC buildings presented in Fig. 2 (a) reveal all data distributed widely, however the values for microtremor higher than 4% are comparatively small. In Fig. 2 (b), many data exist between 0.1 and 0.6 s in the primary natural period T_1 and the damping ratio h_1 decreases that corresponds to an increase in T_1. The regression curve for earthquake observation is higher than those of for microtremor and forced excitation.

3. Study based on earthquake observations

The analysis in Chapter 1 focused on grasping the entirety of the data and examining the amplitude dependence of minute to large amplitudes of information. In this chapter, from the perspective of understanding both the natural period and the damping ratio at the time of a large earthquake, 59 data sets from buildings in the Tohoku earthquake were selected from a total of 382 data. The results of a trend analysis of the natural period and the damping ratio for these data are presented based on [5].

3.1 Observation data and analysis policy

The target observation data was obtained from a total of 59 buildings during the mainshock of the Tohoku earthquake. The number of S buildings is 13, the sum of RC and SRC buildings (hereafter collectively referred to as RS/SRC buildings) is 46. Table 1 presents the specifications. The number of data is about twice (110) the number of buildings, because the data from the short-side and long-side directions are treated separately in the analysis. Except for some building the primary natural period and the damping ratio at the beginning and end of the earthquake (hereafter referred to as beginning time and end time, respectively) are obtained for the purpose of examining the fluctuation of the vibration characteristics before and after the earthquake. As is evident from the range of building heights (H), the structures from where the observation records were obtained vary from high-rise to low-rise buildings.

The range of the maximum drift angle is widely distributed from a small deformation region of less than 1/1000 to a large deformation region close to 1/100. The drift angle during the beginning time and the end time is small. Here, the analysis is conducted using the values of the natural period and the damping ratio for both the beginning and end times.

Table 1 Specification of observation data

Specification of data		**Building type**	
		S	**RC/SRC**
Number of buildings		13	46
Number of data (Total of short- and long-side data)		23	87
Range of height (m)		29.8–256.0	7.5–135.7
Range of natural period (s)	At the beginning	0.69–4.28	0.12–0.71
	At the end	0.95–4.51	0.12–3.10
Range of damping ratio (%)	At the beginning	0.2–5.5	0.5–30.0
	At the end	0.5–5.5	1.0–23.6
Range of maximum drift angle ($\times 10^{-3}$)		0.3–7.7	0.1–9.4

3.2 Natural period

Fig. 3 presents the relationship between the building height (H) and the primary natural period (T_1). To understand the trend at the beginning and end of the earthquake, (a) is the result from the S buildings, and (b) is the result from the RS/SRC buildings. However, the data from three of the S buildings is excluded from the analysis because the timing at the beginning and end of the earthquake is unknown. In the figure, a regression line ($T = a\,H$) passing through the origin is presented along with the data at the beginning and end of the earthquake. However, the S building with a height of 256 m is excluded from regression because the data is far below (the short-period side) from the other S buildings. In addition, the regression lines (the S buildings: T = 0.02 H; the RS/SRC buildings: T = 0.015 H) studied by the AIJ [1], [2] are added for comparison.

With reference to Fig. 3, at the end of the earthquake, the T value for the same H is about 10% longer than the T value at the beginning for S buildings and about 20% for RS/SRC buildings. Also, when compared with the regression lines by AIJ, the coefficient values of lines at the beginning are larger by 0.04 for S buildings and by 0.05 for RS/SRC buildings.

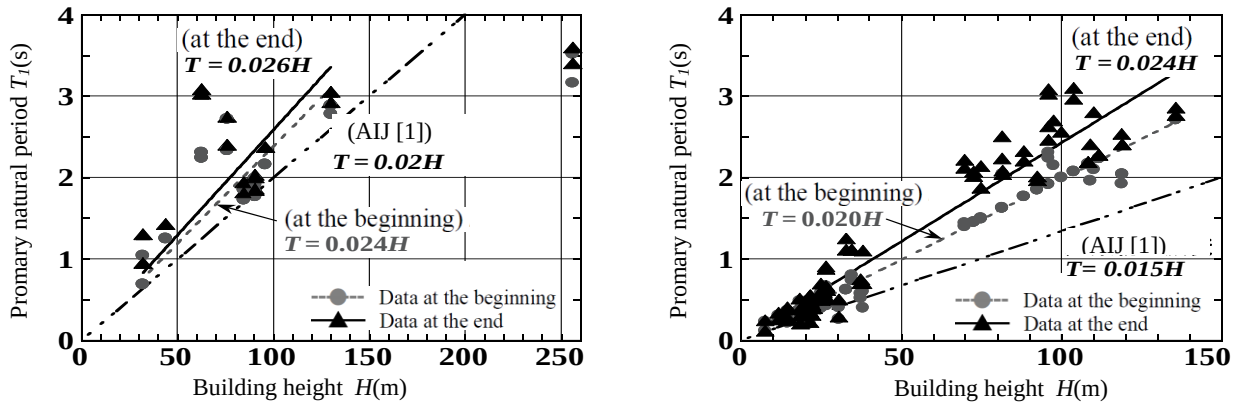

(a) S buildings (b) RC buildings

Fig.3 – Relationship between height and natural period
using observation data in the Tohoku Earthquake

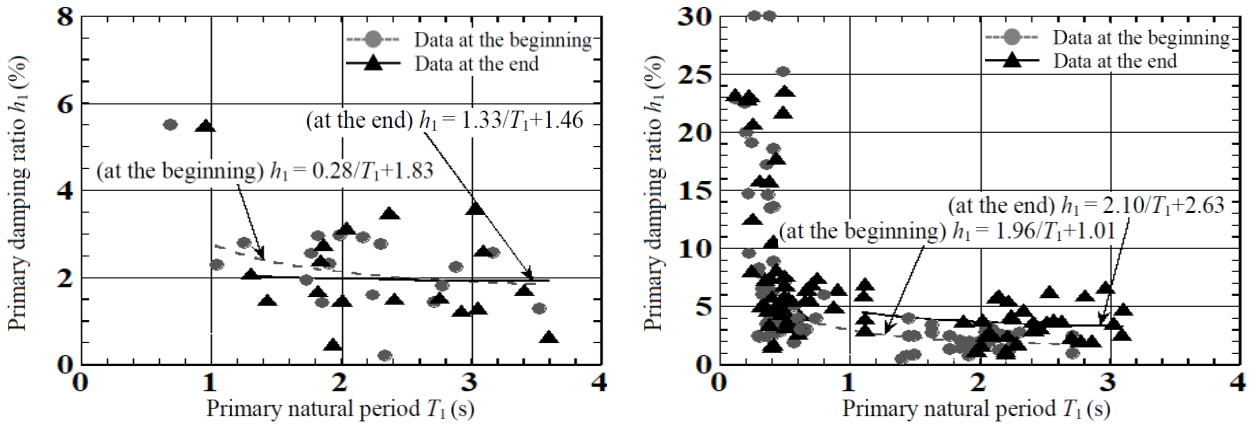

(a) S buildings (b) RC buildings

Fig.4 – Relationship between primary natural period and damping ratio
using observation data in the Tohoku Earthquake

3.3 Damping ratio

Fig. 4 presents the relationship between T_1 and the damping ratio h_1. As in Fig. 3, (a) is the result from S buildings, and (b) is the result from RS/SRC structures. In Fig. 4, the regression lines using Equation (1) for the data at the beginning and end times are also presented.

For the regression, only the data from the period $T > 1$ s are used. As shown in Chapter 2, the damping ratio for low-rise (short-period) buildings varies significantly, whereas the damping ratio for the high-rise (long-period) buildings settles in a comparatively small range. It is considered that this variation of low-rise buildings is mainly attributed to the effects of SSI. Since the foundation and soil types vary between buildings, these differences can be the cause of the damping ratio variations for low-rise buildings. Therefore, this study considers that the damping ratio of the building itself (without the effect of SSI) can be obtained using the data at $T > 1$ s.

A comparison of the regression curves of the data in Fig. 4 reveals no significant difference between the beginning and end times for S buildings; the end time is slightly larger than the beginning. For RC/SRC buildings, from the regression curve (in the region of $T > 1$ s), h_1 tends to settle down to about 2% for S buildings and 2 to 3% for RS/SRC buildings.

3.4 Summary

From the results of the analysis based on the observation data from the Tohoku earthquake shown above, the damping ratio of a low-rise building with a shorter natural period is higher in value and wider in variation; the tendency is particularly remarkable in RS/SRC buildings (Figs. 3 and 4). The same trend was observed in the results from the DB presented in Chapter 2, which is considered to be the effect of the SSI. In the next chapter, the results of the actual DB and the observation data of the Tohoku earthquake are further examined from the viewpoint of the exclusion of the SSI effect.

4. Analysis based on average and standard deviation of damping

In Chapter 2, a trend analysis was conducted using all DB data (382 buildings). In Chapter 3, a trend analysis of natural frequency and damping ratio was conducted for a total of 59 buildings during the Tohoku earthquake. In this chapter, a more quantitative study is conducted using the average (avg.) and standard deviation (σ) of the data whose primary natural frequency is 1 s or more (hereafter referred to as $T_1 \geq 1$ s) for the purpose of evaluating the damping ratio of the building itself—excluding the SSI effect.

4.1 Analysis based on DB data

First, the DB in Chapter 2 is analyzed. Both RC and SRC are treated together as RC/SRC. This is because the number of these data with a value of $T_1 \geq 1$ s is relatively small. As is evident from Figs. 1 and 2, the damping ratio is high for low-rise buildings with small T_1, and the variation is large; the high ratio is thought to be due to the SSI effect. This effect is greatly affected by the type of ground, foundation, and basement, and there are many variations among the observed buildings. Consequently, the damping ratio of low-rise buildings is considered to vary greatly.

Therefore, the damping ratio of the building itself (which excludes the SSI effect) is examined. Table 2 presents the avg. and σ of the damping ratio for the S buildings, whereas Table 3 presents the values for the RC/SRC buildings. In both tables, the values obtained by comparing all data with the data separated by $T_1 \geq 1$ s are presented. Here, $T_1 \geq 1$ s is set as a range in which the SSI effect has almost no impact, but since the range of influence depends on each building's situation, it is not necessarily a strict division and is used only as a guide. In both tables, the coefficient of variation (σ / avg.) of all data is as large as about 0.5 to 0.7 for S buildings and about 0.7 to 0.8 for RC/SRC buildings. This indicates that the damping ratio varies significantly between buildings.

According to Table 2, the avg. of the damping ratio of the S buildings is in the relationship of microtremor $\approx$ forced excitation < earthquake observation. In addition, the σ has a similar tendency. When

comparing all data with the data of $T_1 \geq 1$ s, there is not much difference. This is because nearly 90% of all data are $T_1 \geq 1$ s.

Table 2 Avg. and σ of damping ratio (S buildings)

		All data	**Microtremor**	**Forced excitation**	**Earthquake observation**
Avg. (%)	All data	1.42	1.19	1.22	2.12
	Only $T_1 \geq 1$ s	1.39	1.18	1.09	2.11
	Ratio ($T_1 \geq 1$ s /All)	0.98	0.99	0.89	1.00
σ (%)	All data	1.02	0.73	0.65	1.47
	Only $T_1 \geq 1$ s	1.03	0.73	0.55	1.45
	Ratio ($T_1 \geq 1$ s /All)	1.01	1.00	0.85	0.99
Coefficient of variation	All data	0.72	0.61	0.53	0.69
	Only $T_1 \geq 1$ s	0.74	0.62	0.50	0.69
	Ratio ($T_1 \geq 1$ s /All)	1.03	1.01	0.95	0.99
Number of data	All data	561	187	241	109
	Only $T_1 \geq 1$ s	495	171	195	105
	Ratio ($T_1 \geq 1$ s /All)	0.88	0.91	0.81	0.96

Table 3 Avg. and σ of damping ratio (RC/SRC buildings)

		All data	**Microtremor**	**Forced excitation**	**Earthquake observation**
Avg. (%)	All data	3.18	2.76	2.73	4.09
	Only $T_1 \geq 1$ s	2.00	1.71	1.47	2.55
	Ratio ($T_1 \geq 1$ s /All)	0.63	0.62	0.54	0.62
σ (%)	All data	2.51	1.97	1.79	3.24
	Only $T_1 \geq 1$ s	1.31	1.01	0.58	1.65
	Ratio ($T_1 \geq 1$ s /All)	0.52	0.51	0.32	0.51
Coefficient of variation	All data	0.79	0.71	0.66	0.79
	Only $T_1 \geq 1$ s	0.66	0.59	0.39	0.65
	Ratio ($T_1 \geq 1$ s /All)	0.83	0.83	0.60	0.82
Number of data	All data	496	217	114	163
	Only $T_1 \geq 1$ s	142	63	25	52
	Ratio ($T_1 \geq 1$ s /All)	0.29	0.29	0.22	0.32

Conversely, in the RC/SRC buildings in Table 3, the relationship of microtremor ≈ forced excitation < seismic observation is viewed as an avg. The σ has the same tendency. When comparing all data with the data of $T_1 \geq 1$ s, there is a large difference in the avg. and the σ, unlike the S buildings. When examining the ratio of the data of $T_1 \geq 1$ s to all the data, the avg. is about 0.6, the σ is about 0.5, and the variation

coefficient is about 0.8. Both the avg. and variation of the damping ratio are small. This is considered to be due to the fact that by narrowing down to $T_1 \geq 1$ s, the damping ratio of the building itself, which has a smaller variation, was obtained. Based on the above, it is considered more effective to obtain the damping ratio of the building itself based on the data of $T_1 \geq 1$ s.

4.2 Analysis based on the Tohoku earthquake data

From the analysis in 4.1, different damping ratios were evaluated for microtremor observation, forced excitation, and seismic observation due to the amplitude dependence of the damping ratio. It is highly likely that the seismic observation data in Table 3 includes nonlinear hysteretic damping by the plasticization of the building due to the strong earthquake, which increased the damping ratio. Therefore, to contribute to the study of the initial damping ratio used in the seismic design, the analysis is conducted on the data at the beginning and end times of the Tohoku earthquake presented in Chapter 3.

First, as in Section 4.1, the damping ratio of the building itself, which does not include the SSI effect, is studied. Tables 4 and 5 present the avg. and σ values of the damping ratio based on all data and the data of $T_1 \geq 1$ s for both S and RC/SRC buildings.

Table 4 Avg. and σ values of damping ratio (S buildings)

	Number of buildings	**Number of data**	**At the beginning**		**At the end**	
			Avg. (%)	**σ (%)**	**Avg. (%)**	**σ (%)**
All data	10※	18	2.31	1.05	2.15	1.19
Data for $T_1 < 1$ s	1	1	5.50	0.00	5.50	0.00
Data for $T_1 \geq 1$ s	10	17	2.12	0.74	1.96	0.89

※The total number of data is different from the sum of T1 < 1 s and $T_1 \geq 1$ s, because one-direction data from one building is T1 <1 s

Table 5 Avg. and σ values of damping ratio (RC/SRC buildings)

	Number of buildings	**Number of data**	**At the beginning**		**At the end**	
			Avg. (%)	**σ (%)**	**Avg. (%)**	**σ (%)**
All data	44	85	6.19	6.69	6.61	5.45
Data for $T_1 < 1$ s	27	54	8.59	7.36	8.47	6.00
Data for $T_1 \geq 1$ s	17	31	2.02	0.86	3.38	1.51

As in 4.1, the difference of the avg. and σ between all data and the data of $T_1 \geq 1$ s is not so significant, because in the S buildings, the number of data of $T_1 < 1$ s is small. However, in the RC/SRC buildings, there is a large difference of the avg. and σ between $T_1 < 1$ s and $T_1 \geq 1$. By narrowing down the data to $T_1 \geq 1$ from these, it is considered that the variation due to the SSI effect was removed, and the property of the damping ratio of the building itself was approached. For RC buildings, the damping ratio tends to increase at the end of the earthquake compared with the beginning. This is believed to be due to the plasticization of the building from the occurrence of cracks and the other damage due to the earthquake. Therefore, it is considered appropriate that the damping ratio used in the design is based on the value at the beginning of the earthquake before plasticization.

However, it is possible that the building was plasticized by another tremor before the Tohoku earthquake, which increased the damping ratio. Ito et al. [2] revealed that the damping ratio at the end of the Tohoku earthquake tended to increase when the Japanese seismic intensity at the building site was 5 (−) or

more. Therefore, the location of each RC/SRC building was examined; the correlation with the earthquake records at that location determined whether or not the building had been shaken by a seismic intensity of 5 (−) or more from completion to the Tohoku earthquake. Table 6 presents the results. In the table, the avg. of untested data with a seismic intensity of 5 (−) or more at T1 ≥ 1 s is 1.89, which is slightly lower than the value for all data at 2.02. This is considered to correspond to the initial damping ratio of RC buildings. From the above examination, the initial damping ratio of both the S and RC/SRC buildings at the beginning of the earthquake, which did not include the SSI effect, was about 2% on avg. and about 0.8% in terms of σ.

Table 6 Avg. and σ of damping ratio with consideration of earthquake experience (RC/SRC buildings)

	Number of buildings	**Number of data**	**At the beginning**		**At the end**	
			Avg. (%)	**σ (%)**	**Avg. (%)**	**σ (%)**
Data for $T_1 \geq 1$ s	17	31	2.02	0.86	3.38	1.51
No seismic intensity of 5 (−) or more before Tohoku earthquake	13	24	1.89	0.78	-	-

5. Proposal of the initial damping ratio for the seismic design

Based on the investigation in Chapter 4, the following section proposes values for the seismic design on the initial primary damping ratio of the RC/SRC buildings and the S buildings for the horizontal direction.

5.1 Initial primary damping ratio for RC/SRC buildings

Table 7 presents the calculated values of (avg.), (avg. −0.5 σ), and (avg. −1.0 σ) of the damping ratio based on the avg. of 1.89 and σ 0.78 in Table 6. Assuming that the damping ratio varies according to the normal distribution, the probability that the given value is on the safe side at (avg.) is about 0.5; at (avg. −0.5 σ), it is 0.7; and at (avg. −1.0 σ), it is 0.85. The values obtained by rounding to the nearest 0.5 increment are also presented in the table. From this value, the proposed initial damping ratio for RC buildings is set to 2.0% to 1.0%, which corresponds to the (avg.) and (avg. −1.0 σ). This study proposes that a ratio of 2.0% is appropriate for application to general buildings with values of 1.5% and 1.0% for important buildings—in accordance with their importance.

Table 7 Proposed initial damping ratio for RC/SRC buildings

	Avg. (%)	**Avg. −0.5 σ（%）**	**Avg. −1.0 σ（%）**
Calculated values	1.89	1.50	1.11
Proposed values	**2.0**	**1.5**	**1.0**
Probability of being on the safe side*1	0.5	0.7	0.85

*1 These probability values are approximated, because the proposed damping value are rounded

5.2 Initial primary damping ratio for S buildings

It is known that the damping ratio of S buildings shows a complicated amplitude dependence compared with the RC/SRC buildings, as presented in Fig. 5 [6]. As an example, Fig. 6 reveals the amplitude dependence of the primary damping ratio of S buildings observed with the large shaking table "E-Defense" [7].

In Fig. 5, at a small amplitude, the damping ratio is also small. The ratio tends to increase (A–B) as the amplitude increases and then decreases from a certain amplitude (B–C). Then, the amplitude further increases from a certain amplitude (C–D). Aquino and Tamura [8] described the properties of A–B using the stick–slip model and attributed the decrease between B and C to frictional damping.

However, there is considerable variation between these properties. Observations of actual buildings [6] also revealed that during the Tohoku earthquake, some buildings demonstrated B–C properties, whereas others did not. Additionally, the amplitudes at points B and C are unclear. The amplitude at point C (average drift angle of the whole building) in Fig. 6 is nearly 3×10^{-3} and 1×10^{-2}, which indicates that there is a significant variation between samples.

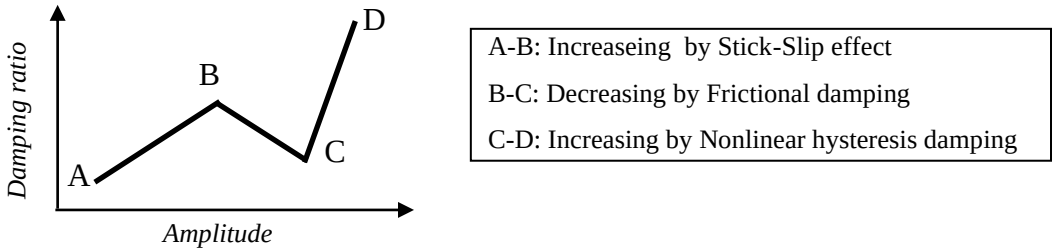

Fig. 5 – Image of relationship between amplitude and damping ratio for S building [5]

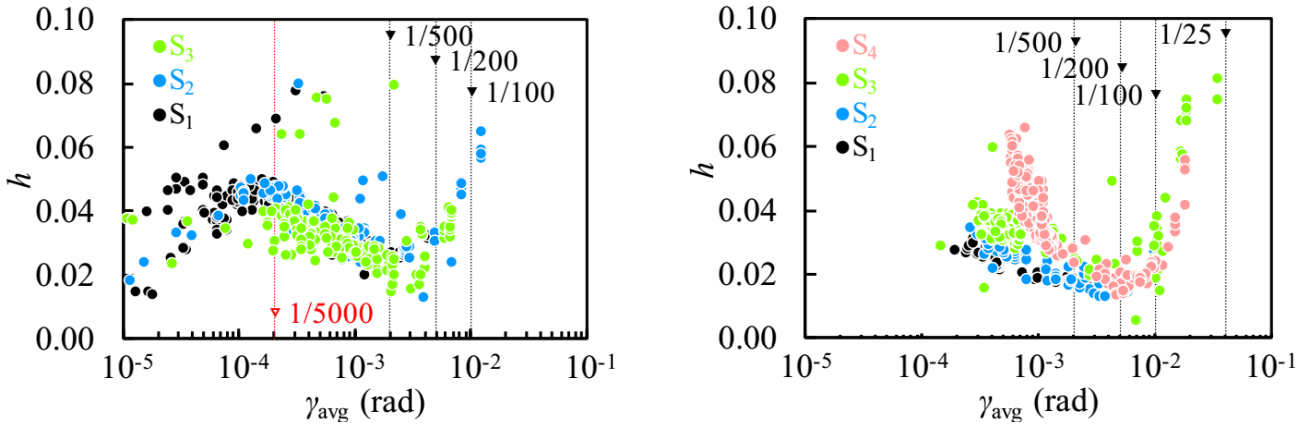

(a) Specimen St.1 (b) Specimen St.3

Fig. 6 – Relationship between primary damping ratio *h* and average drift angle (γ_{avg}) [6]

The data on the damping ratio at point C is extremely limited. However, from the results in Fig. 6 and [6], the average value here is assumed to be about 1.5%. Since the property of a decreasing damping ratio between B and C cannot be expressed by a combination of a general initial damping model and a hysteretic damping model, the initial damping model is reduced to consider this effect.

The trend above the C point is considered to be due to the plasticization of the members. Although the results of the shaking-table experiments for many specimens demonstrate the same trend, it is not found in the observation data from actual buildings discussed in Chapters 2 and 3 and recorded in [6]. This is probably because these data from actual buildings (including the Tohoku earthquake) did not reach an amplitude to induce plasticization after the main members had yielded. This effect is considered to be hysteretic damping and is not considered in the context of initial damping.

As in Section 5.1, the initial damping ratio of S buildings is examined based on Table 8. Unlike the RC/SRC buildings, the difference between the damping ratios at the beginning and end of the earthquake is small for S buildings. Table 8 presents the calculated values of (avg.), (avg. −0.5 σ), and (avg. −1.0 σ) of the damping ratio and the rounded values to the nearest 0.5 increment. From this value, the (avg.) and (avg. −1.0 σ) values of the initial damping ratio of the S building are 2.0% to 1.0%, respectively.

However, since these values are based on the relatively small amplitudes at the beginning and end of the earthquake, they may not include the decreasing trend in the damping ratio between B and C. Therefore, a correction is made to Table 8, and the avg. after the correction is set to 1.5%. Assuming that the value of the σ does not change, the values (avg. −0.5 σ) and (avg. −1.0 σ) are set to 1.0% and 0.5%, respectively (see Table 9).

Table 8 Calculated damping values for S buildings

	Avg. (%)	**Avg. −0.5 σ** (%)	**Avg. −1.0 σ** (%)
Calculated value (at the beginning)	2.12	1.75	1.38
Calculated value (at the end)	1.96	1.53	1.18
Rounded value	2.0	1.5	1.0

Table 9 Proposed initial damping ratio for S buildings (after correction)

	Avg. (%)	**Avg. −0.5 σ** (%)	**Avg. −1.0 σ** (%)
Rounded value	1.5	1.0	0.5
Probability of being on the safe side*1	0.5	0.7	0.85

*1 As the proposed damping values are rounded and corrected, these probability values are approximated

6. Conclusions

In this paper, the initial damping ratio for general S buildings and RC/SRC buildings, which is important for the seismic design, was examined. The main conclusions are as follows:

1) The database compiled by the AIJ contains a large amount of diverse data types. Since damping depends on the amplitude, the damping ratio increases in the order of microtremor < forced excitation < earthquake observation.

2) However, earthquake observation data includes not only the initial damping but also the hysteretic damping that occurs during a large-amplitude quake. For this reason, the damping ratio was examined using the Tohoku earthquake data observed at the beginning of the earthquake.

3) In short-period buildings, the damping ratio varies greatly due to the influence of the SSI. For this reason, the damping ratio of the building itself (which does not include the interaction effect) was examined using data that excluded short periods (in this paper, data with a period of 1 s or more were used).

4) Furthermore, since the damping ratio has a large variation, the study in this paper included not only the average value (avg.) but also the standard deviation (σ).

5) In S buildings, the damping ratio may decrease as the amplitude increases in a certain area. Considering this, the damping ratio of the S building was reduced by 0.5%.

6) Based on the above, the damping ratios appropriate for seismic design are presented below; it is proposed that the ratios are applied according to the importance of the building.

RC/SRC buildings:	(Avg.): 2.0%,	(Avg. −0.5 σ): 1.5%,	(Avg. −1.0 σ): 1.0%
S buildings:	(Avg.): 1.5%,	(Avg. −0.5 σ): 1.0%,	(Avg. −1.0 σ): 0.5%

7. Acknowledgments

This paper is based on some of the research results in the subcommittee of the Architectural Institute of Japan's "Estimation of Damping Mechanism and Its Performance on Buildings" (Supervisor: N. Nakamura). The authors would like to express their gratitude to all those concerned.

8. References

[1] Architecture Institute of Japan (2000): Damping in buildings (in Japanese).

[2] Satake N, Suda K, Arakawa T, Sasaki A, Tamura Y (2003): Damping evaluation using full-scale data of buildings in Japan. *Journal of Structural Engineering ASCE*, 129(4), 470-477

[3] Satake N, Nakamura N (2019): Evaluation of natural period and damping ratio of buildings. *Summary of the 65th National Congress of Theoretical and Applied Mechanics* (in Japanese).

[4] Satake N, Ougiya N, Ito S, Hirata Y, Song S, Shingu K and Shimaoka S (2020): Outline of Database and Regression Analyses on Vibration Damping Data of Full-Scale Buildings and Architecture. *17th World Conference on Earthquake Engineering*, Paper# C003579, Sendai, Japan

[5] Ito S, Nakamura N, Miyazu Y, Kashima T, Sone T, Miyamoto Y (2017): Damping and eigen-period of buildings based on recent information, Part-2 Analysis of observation records and simulation results of buildings during the 3.11 earthquake. *Summaries of technical papers of annual meeting Architectural Institute of Japan* (in Japanese).

[6] Nakamura N, KASHIMA T, MIYAZUY, TOJO T, HIDA T, IIYAMA K and SUZUKI T (2018): Study on Horizontal First and Second Vibration Characteristics of High Rised Steel Buildings Considering Amplitude Dependency. *Journal of Structure and Construction Engineering, AIJ,* 83(753), (In Japanese)

[7] Tojo T, Nakamura N, Kajiwara K, Satake N, Tosauchi Y (2020): Vibration characteristics of steel buildings based on large shaking table tests at e-defense. *17th World Conference on Earthquake Engineering*, Paper# C001291, Sendai, Japan

[8] Aquino, RER and Tamura Y (2013): Structural Damping Estimation for Wind -Resistant Design of 200m-High Steel Office Building Using Stick-Slip Model. Journal of Wind Engineering, JAWE, 38(2, 135)

